Carbohydrate Polymers 91 (2013) 269–276

Contents lists available at SciVerse ScienceDirect

Carbohydrate Polymers

journal homepage: www.elsevier.com/locate/carbpol

# Long-alkane-chain modified *N*-phthaloyl chitosan membranes with controlled permeability

Chao Chen[a,1], Shuming Tao[b,1], Xiaoyun Qiu[a], Xueqin Ren[a,*], Shuwen Hu[a,**]

[a] Department of Environmental Sciences & Engineering, College of Resources and Environmental Sciences, China Agricultural University, Beijing 100193, PR China
[b] Department of Plant Nutrition, College of Resources and Environmental Sciences, China Agricultural University, Beijing 100193, PR China

ARTICLE INFO

*Article history:*
Received 29 June 2012
Received in revised form 10 August 2012
Accepted 11 August 2012
Available online 19 August 2012

*Keywords:*
Chitosan
Acylation
*N*-phthaloylation
Hydrophobicity
Controlled permeability

ABSTRACT

A series of *N*-phthaloyl acylated chitosan membranes with controlled permeability were synthesized by the regioselective protection of the chitosan amino groups as the corresponding phthalimides followed by reaction with the long-chain dodecanoyl chloride. Fourier transform infrared (FT-IR) and $^1$H nuclear magnetic resonance ($^1$H NMR) analysis suggested that the degree of substitution (DS) ranged from 2.8 to 3.6. Contact angles, water retention values and mechanical examinations demonstrated that the hydrophobicity and mechanical properties of the membranes were all improved significantly following the modifications, together with their solubility in many organic solvents. Thermal weight change analysis demonstrated that a higher DS provided enhanced thermal properties. The controlled permeability of the membranes was determined by measuring the diffusion of urea, and the amount of urea released decreased significantly with increasing DS. The comprehensive properties of the membranes could be tuned by regulating their DS values as required.

© 2012 Elsevier Ltd. All rights reserved.

## 1. Introduction

In the last decades, significant advances have been made in the development of controlled-release matrices for agrochemicals, such as fertilizers, as a consequence of the increasing demand for site-specific target chemicals capable of providing a sustained delivery of material (Abedi-Koupai, Varshosaz, Mesforoosh, & Khoshgoftarmanesh, 2012; Wang & Alva, 1994). Membranes (Chen, Ding, & Qin, 2012; Kawashima et al., 2011), fibers (Loh, Peh, Liao, Sng, & Li, 2010; Lonescu, Lee, Sennett, Burdick, & Mauck, 2010), and hydrogels (Sutton et al., 2009; Thornton, Mart, Webb, & Ulijn, 2008) are the most developed platforms for target delivery. Biodegradable polymeric materials are understandably preferred candidates for the development of controlled and slow-release agrochemicals (Han, Chen, & Hu, 2009; Li, Li, & Dong, 2008).

Chitosan is one of the most important partially deacetylated derivatives obtained from chitin and the second most abundant aminated polysaccharide on the earth (Muzzarelli, 1996). Chitosan is an amino polysaccharide possessing unique properties, such as biocompatibility and biodegradability (Muzzarelli, 2009). Furthermore, chitosan has been widely applied as a slow-release material in fertilizers and other agrochemicals (Wu & Liu, 2008).

Although chitosan is an attractive biomacromolecule, it is insoluble in most common organic solvents and water, which greatly limits its applications in a variety of different fields. In addition, chitosan is a rigid and brittle material, as a consequence of its abundant inter- and intra-molecular hydrogen bonding interactions which have an adverse impact on its processability and have severely limited the development of chitosan membranes (Ma, Yang, Kennedy, & Nie, 2009; Xiao, Feng, & Huang, 2007). Chitosan, however, contains hydroxyl groups and highly reactive amino groups and has been successfully modified by a series of chemical reactions including *N*-alkylation (Kurita, Mori, Nishiyama, & Harata, 2002b), *N*-acylation (Hirano, Zhang, Chung, & Kim, 1999; Morimoto et al., 2011), and *N*-carboxyalkylation (Sreedhar, Aparna, Sairam, & Hebalkar, 2007). Following these chemical modifications, the solubility of chitosan in common organic solvents was enhanced, which improved the properties of the chitosan membranes (Osifo & Masala, 2010).

A long-chain acyl chloride was used to modify chitosan and the resulting acylated material exhibited excellent solubility in common organic solvents and good film formability (Fujii, Kumagai, & Noda, 1980; Zong, Kimura, Takahashi, & Yamane, 2000). Unfortunately, however, the acylation of chitosan requires heterogeneous conditions, involving a time consuming soaking period of the material in anhydrous pyridine for several days prior to the acylation reaction. Furthermore, an extremely long reaction time is required

* Corresponding author. Tel.: +86 010 62733407; fax: +86 010 62731016.
** Corresponding author. Tel.: +86 010 62731255; fax: +86 010 62731016.
*E-mail addresses:* renxueqin@cau.edu.cn (X. Ren), shuwenhu@cau.edu.cn (S. Hu).
[1] The first and second authors contributed equally to this work.

0144-8617/$ – see front matter © 2012 Elsevier Ltd. All rights reserved.
http://dx.doi.org/10.1016/j.carbpol.2012.08.042

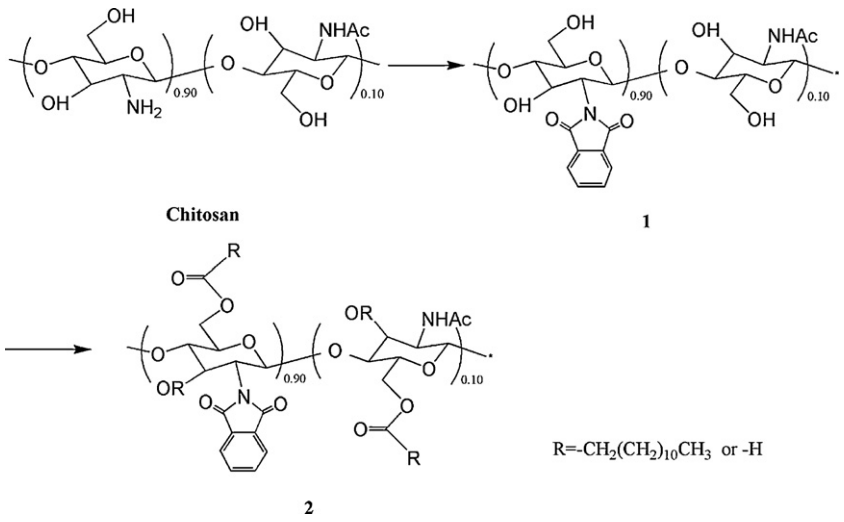


**Scheme 1.** Synthetic route for the construction of *N*-phthaloyl acylated chitosan. Reagents and conditions: (1) phthalic anhydride, DMF/water, 120 °C, 8 h; (2) dodecanoyl chloride, DMF/pyridine, 6 h.

together with the requirement for a significant excess of the acylating reagent. To conduct the acylation reactions efficiently and readily, the availability of chitosan precursors is critical. Herein, we report a novel method for the preparation of *N*-phthaloyl chitosan which involves an initial *N*-protection step followed by the introduction of long-chain acyl chloride units (Kurita, Akao, Kobayashi, Mori, & Nishiyama, 1997; Kurita, 1998). In particular, the current work involved the swelling of *N*-phthaloylated chitosan intermediates in organic solvents to enable the subsequent synthesis of *N*-phthaloyl acylated chitosan. The reaction conditions were milder, simpler, and more efficient, and it was envisaged that the DS values would be higher and that they could be adjusted by regulating the dosage of dodecanoyl chloride. It is worthy of note that the *N*-phthaloyl group can be hydrolyzed using anhydrous hydrazine to provide the free amino acylated chitosan as required (Tao, Pang, Chen, Ren, & Hu, 2012). It was envisaged that this product would have better physical characteristics, including an enhanced level of solubility in organic solvents, film formability, flexibility, and controlled permeability.

## 2. Materials and methods

### 2.1. Materials

Chitosan derived from crab shells was purchased from Goldshell Biochemical Co. Ltd. (Taizhou, China). The degree of deacetylation was determined by $^1$H NMR to be 90% and the material was used without further purification. Dodecanoyl chloride was purchased from Tokyo Chemical Industry Co. Ltd. (Tokyo, Japan) and was used without further purification. All other chemicals were purchased from Sinopharm Chemical Reagent Co., Ltd. (Shanghai, China). *N*,*N*-dimethylformamide (DMF) was stirred with $CaH_2$ (50 g/L) overnight, followed by vacuum distillation at 20 mmHg ($2.7 \times 10^3$ Pa) prior to dry the solvent. Phthalic anhydride was purchased as the analytical grade and used without further purification.

### 2.2. Synthesis and film forming of acylated chitosan

The synthetic procedure used for the construction of acylated chitosan is depicted in Scheme 1. The *N*-phthaloylation of chitosan was conducted in accordance with a procedure previously reported in the literature (Kurita, Ikeda, Yoshida, Shimojoh, & Harata, 2002a). Briefly, to a solution of phthalic anhydride (2.76 g, 18.60 mmol) in a mixture of unpurified DMF and distilled water (20 mL, 95:5, v/v) was added chitosan (1.0 g) and resulting the mixture was heated with stirring at 125 °C under nitrogen for 8 h. Upon completion of the reaction, the resulting pale tan mixture was cooled to room temperature and poured into ice water. The resulting precipitate was collected by filtration and subsequently suspended in methanol (200 mL) at room temperature for 1 h and filtered. This process was repeated 3 times to remove all of excess phthalic anhydride. The product was dried under vacuum at 80 °C overnight to give 1.6 g of the desired *N*-phthaloylated chitosan.

*N*-phthaloylated chitosan (1.0 g) was suspended in a mixture of DMF (30 mL) and pyridine (40 mL) and the mixture was stirred for 12 h under nitrogen at 125 °C to allow for sufficient swelling of the material. The mixture was then cooled in an ice-salt bath and a solution of dodecanoyl chloride (7.13 mmol) in chloroform (2 mL) was added in a drop-wise manner over a period of 1 h. The resulting mixture was stirred for 6 h at room temperature and a heterogeneous aggregation (deep yellow in color) was observed in the mixture. The mixture was poured into a mixture ice water and methanol (300 mL, 2:1, v/v) and the resulting precipitated product was collected by filtration. The product was then suspended in methanol (300 mL), stirred at room temperature for 4 h and collected by filtration. The product was then dissolved in ethyl acetate and poured onto a tetrafluoroethylene plate and then dried under vacuum at 40 °C overnight to give the desired *N*-phthaloyl acylated chitosan membranes (2.18 g). For the fabrication of *N*-phthaloyl acylated chitosan membranes with lower DS values, similar methods of preparation were used and the amounts of dodecanoyl chloride were changed. For example, when 6.58 and 6.03 mmol of dodecanoyl chloride were used, the DS values of the resulting *N*-phthaloyl acylated chitosan membranes were 3.3 and 2.8, respectively.

### 2.3. FT-IR spectroscopy

FT-IR spectra were recorded on a Nicolet NEXUS-470 Spectrometer (Thermo Fisher Scientific, USA) from KBr pellets at room temperature. Samples (2 mg) were thoroughly ground with KBr and pellets were prepared using a hydraulic press under a pressure of 600 kg/cm$^2$. All spectra were recorded with an accumulation number of 32 scans and a resolution of 8 cm$^{-1}$.

### 2.4. $^1H$ NMR spectroscopy

$^1H$ NMR spectra were carried out on a BRUKER DPX 300 MHz spectrometer (Bruker, Germany). Chitosan was dissolved in a mixed solvent system of $CD_3COOD$ and $D_2O$. The *N*-phthaloyl acylated chitosan derivates were dissolved in $CDCl_3$ and tetramethylsilane (TMS) was used as an internal reference.

### 2.5. Solubility test

The solubility of chitosan and the *N*-phthaloyl acylated chitosan derivatives in organic solvents, including ethanol, DMF, trichloromethane, pyridine, and acetone were tested at a concentrations of 10 mg/mL at 25 °C.

### 2.6. Mechanical properties

The *N*-phthaloyl acylated chitosan films were cut into dumbbell-shaped samples. Four tests were performed at room temperature on each of the films using an electronic universal testing machine C43 (Shenzhen, China) at a stretching speed of 2 mm/min. The characteristic parameters of the dumbbell-shaped samples were a gauge length of 15 mm, a width of 5 mm and a thickness of 60 μm.

### 2.7. Thermo-gravimetric analysis (TGA)

Thermal weight change analysis was carried out using a TGA Q50 V20.6 Build 31 from TA Instruments (New Castle, USA) to measure the amount and rate of change in the weight of the films as a function of temperature. The samples (around 5.5 mg) were tested in open aluminum pans under a $N_2$ atmosphere, with a gas flow rate of 40 mL/min. The samples were heated in the furnace up to 600 °C at a heating rate of 10 °C/min in $N_2$. The percentage of weight loss was plotted against the temperature.

### 2.8. Water retention values (WRVs)

For water retention values experiments, the chitosan and *N*-phthaloyl acylated chitosan membranes with different DS values were cut into small pieces of equal size and weight and subsequently soaked in distilled water for 7 days, and sampling was performed per 24 h during these times. The surface water was carefully wiped off the sample with tissue paper prior to weighing (Qiu, Tao, Ren, & Hu, 2012). All the procedures were conducted at room temperature and the WRVs were calculated as the amount of absorbed water related to dry film mass as the following equation:

$$\text{WRVs}\,(\%) = \frac{W_t - W_0}{W_0} \times 100 \quad (1)$$

where $W_t$ is the total weight of the membrane at time $t$ and $W_0$ is the initial mass of the membrane. Each test was performed in triplicate with the results subsequently being averaged.

### 2.9. Contact angle measurement

Contact angles were determined using the pendant drop method with a water drop of 3 μL and an optical contact angle meter SL 100B from Kino Information Technology Co., Ltd. (Shanghai, China) at ambient temperature and humidity. All contact angles were measured on both sides of the drop using the ellipse-fitting calculation method. The contact angle ($\theta$) can be expressed as the following equation:

$$\theta = \arctan\left(\frac{2H}{D}\right) \quad (2)$$

where $D$ is the width of the water drop and $H$ is the height of the water drop. Each of the reported contact angles in the current study represents the average value from a minimum of four measurements.

### 2.10. Determination of permeability of urea

The determination of the permeability of urea was conducted on a Transdermal Diffusion Device TK-6H from Shanghai KaiKai Science and Technology Trade Ltd. Co. (Shanghai, China), which was made up of six diffusion cells attached to a multi-stirrer with clamps (Qiu et al., 2012). Each diffusion cell consisted of two detachable glass compartments with two sampling inlets, a stirrer and an interlayer with a heated outer layer. Films with an average thickness of 60 μm were allowed to soak in distilled water overnight prior to use and cut into pieces with diameters of approximately 30 mm. The film being studied was sandwiched between two compartments, one of which contained a saturated urea solution (20 mL) and the other distilled water which were separated by a 5.5 cm diameter membrane containing the materials being studied. The urea solution was maintained in a saturated state throughout the experiment by the addition of urea granules. The interlayer of each compartment was connected to a thermostatic water-circulator bath from Shanghai Bilon Instruments Co. Ltd. (Shanghai, China) and the experiments were conducted with circulated water at a constant flow rate of 4 L/min at 30 °C and a stirring speed of 200 rpm. Urea permeated from the donor cell into the receiving cell as a consequence of the concentration gradient across the films between the two cells. The urea content in the receiving cell was sampled every 1 h for UV analysis and an aliquot of distilled water (20 mL) was added to replenish what had been lost by the sampling procedure. The urea concentration was determined by UV according to the chromogenic reaction of urea with *p*-dimethylaminobenzaldehyde at a wavelength of 426 nm (Zou, Wang, Dai, Zhou, & Ma, 2006). The tests were performed in triplicate with the average result being reported.

## 3. Results and discussion

In conventional methods of acylated chitosan, the reaction conditions were tedious and critical, such as: long-period soaking about 2–8 days in organic solvents; evaporation of solvents under reduced pressure later; high reflux temperature; and excessive amount of acyl chloride (about 30–50 mmol react with 1 g chitosan) (Fujii et al., 1980; Ma et al., 2009; Zong et al., 2000). While in our modified method, *N*-phthaloylated chitosan does not require the long-period soaking process to fully swell and can react directly with acyl chloride at room temperature with just small amount reagent (only about 6 mmol).

The possible mechanism is that the reaction between phthalic-anhydride and the $-NH_2$ group of chitosan destroyed the inter- and intra-molecular hydrogen bonding interactions, plus, the lipophilic groups enabled the whole acylation process easier.

### 3.1. Chemical structure analysis

The FT-IR spectra of chitosan and the *N*-phthaloyl acylated chitosans with different DS values are shown in Fig. 1(A). The typical absorptions of chitosan were observed at 3448, 1659, and 1599 $cm^{-1}$ and were attributed to the carbonyl stretching and N—H bending vibrations in accordance with other work published in the literature (Cardenas & Miranda, 2004). A comparison of the spectra of *N*-phthaloyl chitosan (curve b) and chitosan (curve a) revealed that the peaks at 1659 and 1599 $cm^{-1}$ in curve b disappeared following the *N*-phthaloylation process (Tao et al., 2012). At the same

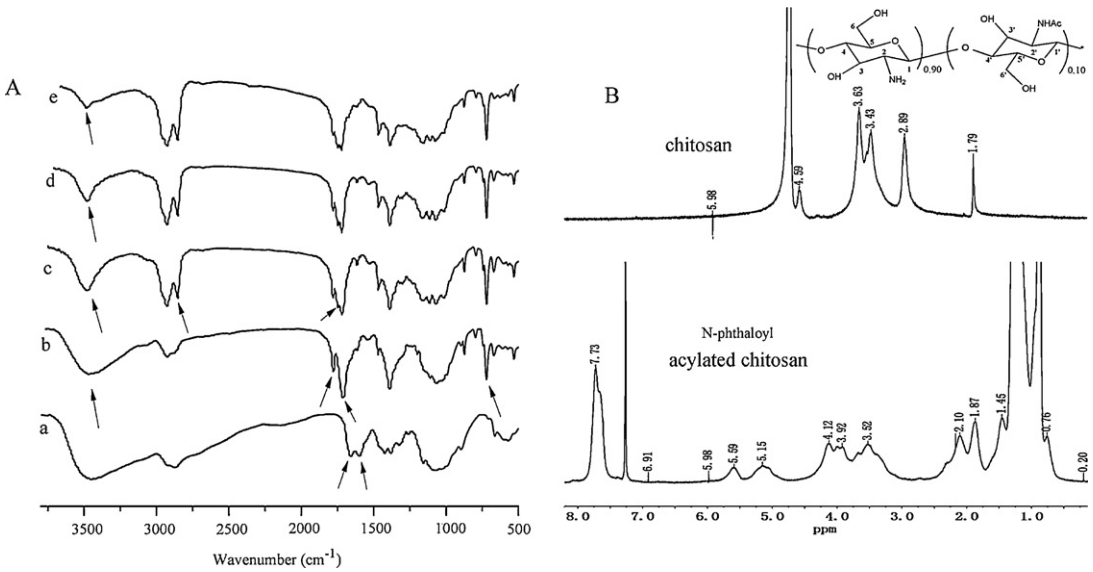


**Fig. 1.** (A) FT-IR spectra of (a) chitosan; (b) *N*-phthaloyl chitosan; (c) *N*-phthaloyl acylated chitosan, DS = 2.8; (d) *N*-phthaloyl acylated chitosan, DS = 3.3; (e) *N*-phthaloyl acylated chitosan, DS = 3.6 and (B) $^1$H NMR spectra of chitosan and *N*-phthaloyl acylated chitosan.

time, new peaks appeared at 1776 and 1712 $cm^{-1}$ that were characteristic of the imide C=O stretching vibration of the *N*-phthaloyl chitosan resulting from the reaction between phthalic-anhydride and the $-NH_2$ groups of chitosan. Another prominent peak at 721 $cm^{-1}$ was assigned to the bending vibrations of $-CH_2$ groups in the phthalic ring (Topacli et al., 2008), which demonstrated that the *N*-phthaloylation reaction was successful. A comparison of the *N*-phthaloyl chitosan with *N*-phthaloyl acylated chitosan (curves c–e) revealed a new peak at 1747 $cm^{-1}$ which was attributed to the bending vibration of the ester groups (—C=O) resulting from the acylation reaction between lauryl chloride and *N*-phthaloylated chitosan (Wang, Lian, Wang, Jin, & Liu, 2012). Other peaks at 2929 and 2857 $cm^{-1}$ were assigned to the asymmetrical and symmetrical bending vibrations of the methylene groups following the introduction of long chains in the acylation reaction. A broad band around 3448 $cm^{-1}$ was assigned as the stretching vibration of the inter- and intra-molecular hydrogen bonds from the $-NH_2$ and —OH groups of the chitosan molecules (Van de Velde & Kiekens, 2004; Zhao, Zheng, Wang, Zhang, & Han, 2012). The intensity of the band was observed to weaken with increasing DS value suggesting the $-NH_2$ groups had been transformed into the corresponding phthalimide groups and the —OH groups into the corresponding acetyl esters. The relative intensities of the absorbance of the $COO^-$ groups (1747 $cm^{-1}$) depended on the DS values. Taken together, this data indicated that *N*-phthaloyl acylated chitosan with different DS values had been successfully prepared.

Representative $^1$H NMR spectra of chitosan in $CD_3COOD/D_2O$ and *N*-phthaloyl acylated chitosan in $CDCl_3$ are shown in Fig. 1(B). The resonance at 1.78 ppm was assigned to the $-CH_3$ groups of the acetamido residue, and the signal at 2.89 ppm corresponded to $H_2$ and $H_{2'}$. The multiplets from 3.4 to 4.6 ppm corresponded to $H_3$–$H_6$ resonances. The degree of deacetylation was found to be 90% and was calculated from Eq. (3) using the intensity values of the integrals (Hiral, Odani, & Nakajima, 1991).

$$D_{deac} = \left[1 - \frac{(1/3)I_{CH_3}}{(1/6)I_{H_2-H_6}}\right] \times 100\% \quad (3)$$

In which, $I_{CH_3}$ is the integral intensity of $CH_3$ residue, and $I_{H_2-H_6}$ is the integral intensity of $H_2$–$H_6$ protons.

Compared to chitosan, the $^1$H NMR spectra of the *N*-phthaloyl acylated chitosan contained a variety of significantly different resonances which corresponded to the incorporation of the *N*-phthaloyl and *O*-acyl groups. Signals observed from 7.5 to 8.0 ppm were attributed to the protons of the phthalic ring (Ma et al., 2011), whereas the broad multiplet peaks observed from 1.26 to 1.45 ppm and the peak typically seen at 0.88 ppm, which were consistent with the presence of $-CH_2$ and $-CH_3$ groups, respectively, were attributed to the dodecanoyl chains from the esterification reaction with dodecanoyl chloride. Other signals observed from 3.4 to 5.6 ppm were assigned to the protons of chitosan and were consistent with other data reported in the literature (Ma et al., 2009). The DS values of the acylation were calculated from the $^1$H NMR spectra based on the molar ratio of $-CH_3$ group resonance (0.88 ppm) to the phthalic ring resonances (7.5–8.0 ppm).

### 3.2. Surface appearance of membranes in solvents

Water was used to characterize any changes in the surface morphologies following a period of soaking in solvent. Changes in the surface appearance with time and a comparison of the changes in the surface appearances of chitosan and *N*-phthaloyl acylated chitosan membranes with time are shown in Fig. 2. It is clear from the figure that the chitosan membrane decreased in size dramatically at the beginning of the soaking process and subsequently gradually inflated in size. The shape of the chitosan membrane clearly changed with time because chitosan possesses a high level of hygroscopicity arising from the interactions between its hydroxyl groups and water. In contrast, the *N*-phthaloyl acylated chitosan membrane remained in sheet from over the same time period and did not change because the hydrophilic hydroxyl and amine groups were substituted with a long hydrophobic hydrocarbon chains and a lipophilic aromatic unit, respectively, which made the *N*-phthaloyl acylated chitosan highly water-resistant.

When a sample of chitosan was dissolved in a dilute solution of aqueous acetic acid (1%, v/v), a viscous solution formed instantly. In contrast, when the modified chitosan was dissolved in DMF at the same concentration, the viscosity of the solution was much lower. Following a film-forming test based on the film-casting method, the chitosan membrane was observed to be rigid and tough, whereas the *N*-phthaloyl acylated chitosan membrane was soft and elastic at room temperature. These results indicated that the *N*-phthaloyl acylated chitosan possessed a superior level of film formability and

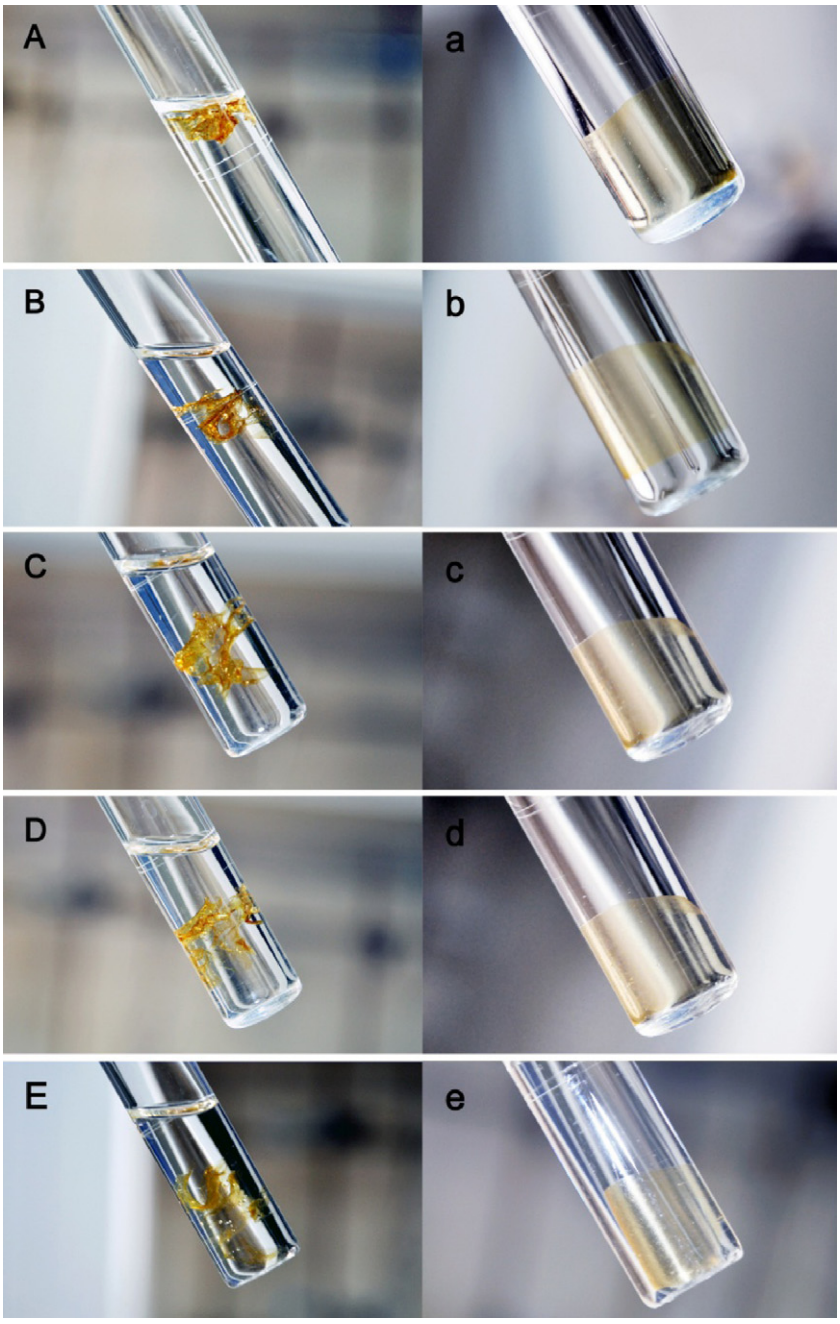


**Fig. 2.** Surface appearance of chitosan following (A) 0 min; (B) 1 min; (C) 5 min; (D) 1 h and (E) 24 h of being soaked in deionized water. Acylated chitosan membranes following (a) 0 min; (b) 1 min; (c) 5 min; (d) 1 h and (e) 24 h of being soaked in deionized water.

flexibility relative to that of chitosan, and these are important features for a controlled-release material to possess.

### 3.3. Solubility test

Chitosan cannot dissolve in water or organic solvents because of its strong and extensive inter- and intra-molecular hydrogen bonding interactions. In contrast, the *N*-phthaloyl acylated chitosan showed excellent solubility in non-polar solvents such as halogenated hydrocarbons and aromatic solvents but poor solubility in polar solvents such as water and ethanol. Table 1 illustrates the solubility of chitosan and its derivatives. The solubility in organic solvents increased as the DS value increased. These results demonstrated that as the number of hydrophobic benzene groups and carbon chains being introduced into chitosan increased, the number of hydrophilic amino and hydroxyl groups decreased, which prevented the formation of intra- and inter-molecular hydrogen bonding interaction between the amino and hydroxyl groups of chitosan. As a result, the solubility of the associated

**Table 1**
Solubility of (A) chitosan; (B) acylated chitosan, DS = 2.8; (C) *N*-phthaloyl acylated chitosan, DS = 3.3 and (D) *N*-phthaloyl acylated chitosan, DS = 3.6. △: insoluble; ○: soluble; □: partially soluble or highly swelled.

| | Ethanol | DMF | Trichloromethane | Pyridine | Acetone |
|---|---|---|---|---|---|
| A | △ | △ | △ | △ | △ |
| B | △ | ○ | □ | □ | □ |
| C | △ | ○ | ○ | ○ | ○ |
| D | △ | ○ | ○ | ○ | ○ |

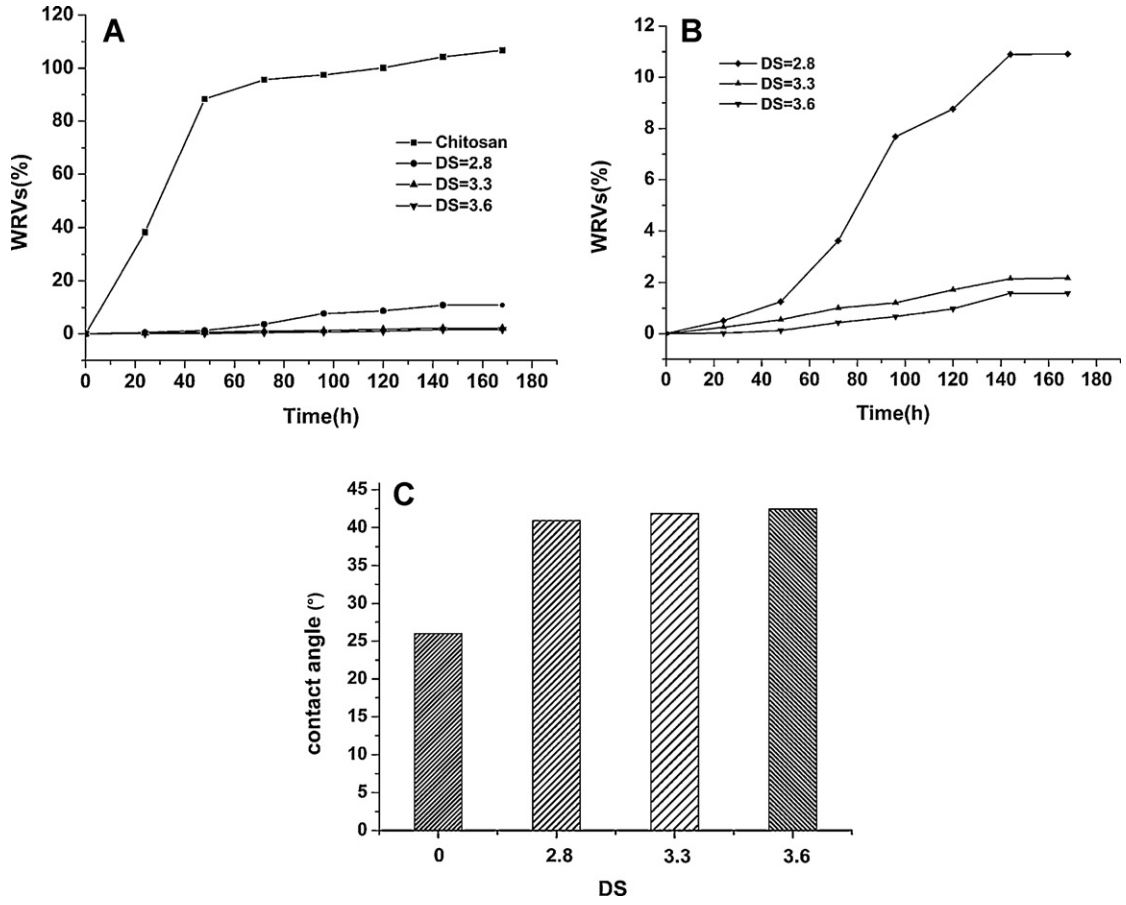


**Fig. 3.** WRVs (A) chitosan and *N*-phthaloyl acylated chitosan membranes with different DS values; (B) *N*-phthaloyl acylated chitosan membranes with different DS values, magnification of A and (C) contact angles of chitosan and *N*-phthaloyl acylated chitosan membranes with different DS values.

chitosan materials in common organic solvents was dramatically improved (Kurita et al., 2002b; Liu, Li, Liu, & Fang, 2004).

### 3.4. Measurement of hydrophobicity

The WRVs and contact angles were examined (Fig. 3) to illustrate the influence of acylation on the hydrophobicity properties of chitosan and its derivatives. Chitosan exhibited a high hygroscopicity because of the interactions between its amino and hydroxyl groups with water molecules. The WRV of chitosan was more than 106% after 7 days, whereas the WRV of *N*-phthaloyl acylated chitosan was less than 11% following the same time period. The WRV profile decreased with an increasing DS value which indicated that the hydrophobicity of the *N*-phthaloyl acylated chitosan membranes was improved with the increasing DS value.

To further characterize the hydrophobic/hydrophilic behavior of the materials, the contact angle measurement was employed. It is clear from Fig. 3(C) that the contact angles increased from 25.8° to 42.9° when the DS value increased from 0.0 to 2.8, providing a clear demonstration that the hydrophobicity of *N*-phthaloyl acylated chitosan was much better than that of chitosan, and that the increase in the value of the contact angles corresponded well with the WRVs. This result can be understood in terms of the fact that the acylated chitosan possessed far fewer hydroxyl groups than

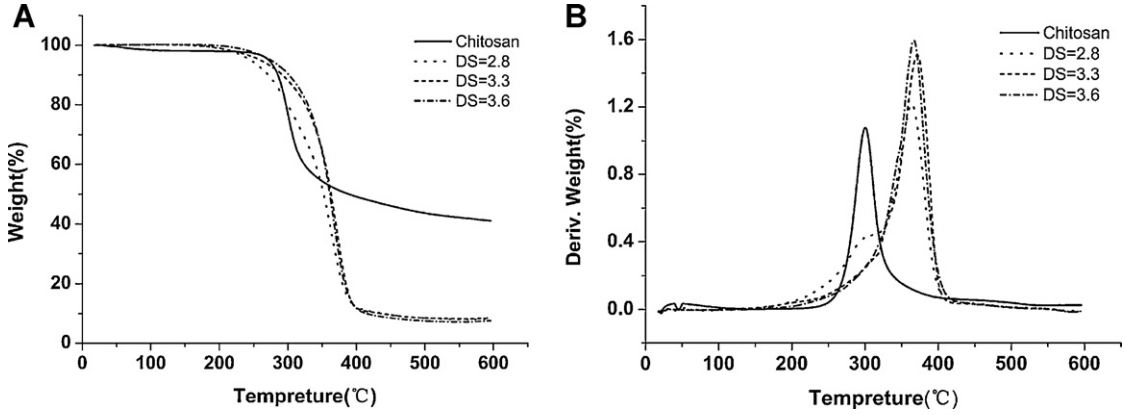


**Fig. 4.** (A) TGA thermograms of chitosan and *N*-phthaloyl acylated chitosans with different DS values and (B) DTG curves of chitosan and *N*-phthaloyl acylated chitosans with different DS values.

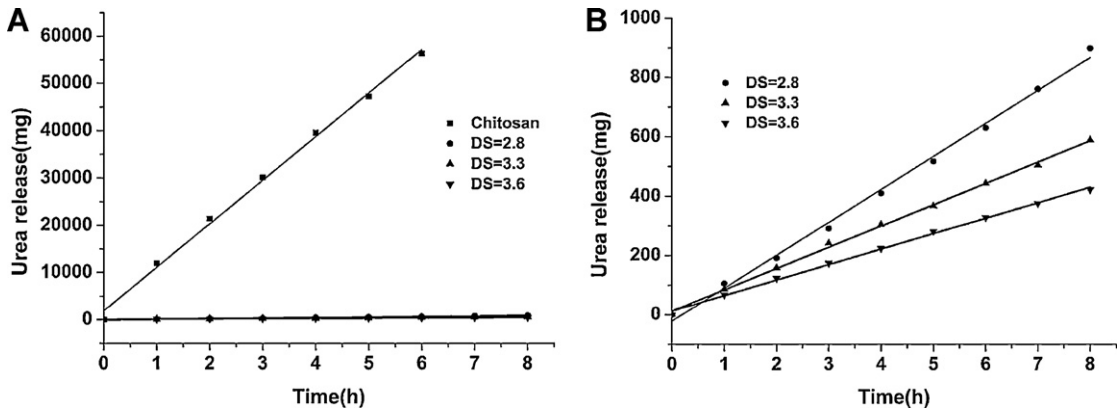


**Fig. 5.** Accumulated permeated urea from (A) chitosan and *N*-phthaloyl acylated chitosan membranes with different DS values and (B) *N*-phthaloyl acylated chitosan membranes with different DS values, magnification of A.

chitosan. The polarity in these compounds would therefore be relatively reduced as a consequence of the incorporation of the long hydrocarbon chains to the main chain of chitosan (Cunha et al., 2008).

### 3.5. Mechanical properties

Table 2 shows the mechanical properties of chitosan and *N*-phthaloyl acylated chitosan. The tensile strength and Young's modulus of the chitosan and *N*-phthaloyl acylated chitosan membranes ranged from 24.6 to 3.75 MPa and 1.980 to 0.157 GPa, respectively. These results indicated that the acylation reaction significantly reduced the tensile strength and Young's modulus of chitosan probably because of the changes in the molecular arrangement. Native chitosan shows a highly ordered and highly crystalline molecular structure because of its extensive intra- and inter-molecular hydrogen bonding interactions (Feng, Liu, Zhao, & Hu, 2012). Following the introduction of a relatively small amount of long-chain alkanes, the crystallinity was of the parent chitosan was destroyed, leading to reduction in the tensile strength and Young's modulus. Further increases in the DS value of the *N*-phthaloyl acylated chitosan membranes, however, a new mode of crystallinity was created by the lengthy alkane side chains which manifested itself in an increased tensile strength and Young's modulus. These results corresponded well with an earlier report from the literature in which an increase in the number of long chains led to an increase in the crystallinity (Tien, Lacroix, Ispas-Szabo, & Mateescu, 2003). These results suggested the mechanical properties of the membranes could be tuned by regulating the DS values of the *N*-phthaloyl acylated chitosan as required. Thus, we can optimize the modified chitosan film to posses the appropriate flexibility and tensile strength required for use in a controlled-release matrix.

### 3.6. TGA analysis

The TGA and DTA curves for chitosan and *N*-phthaloyl acylated chitosan are shown in Fig. 4. For chitosan, the TGA trace showed two stages of weight loss. The first stage occurred at 50–200 °C with a weight loss of approximately 1.8%, which was consistent with the loss of residual water from the material (Huang, Pal, & Moon, 1999). The second stage involved a sharp and considerable weight loss at 200–300 °C with a total weight loss of 52%, which was attributed to the decomposition of chitosan (Ma et al., 2009). The *N*-phthaloyl acylated chitosan with different DS values showed a similar degradation stage between 200 and 400 °C, which reached a maximum at about 360 °C with a total weight loss of 90% which attributed to the decomposition of the polymer (Remant Bahadur et al., 2006). From the percentage weight loss in the TGA curve, it is clear that the thermal stability of *N*-phthaloyl acylated chitosan was weaker than that of chitosan, although the shift to higher temperature was observed as a consequence of an increase in the thermal stability of the material resulting from the in the number of acylated chains in the *N*-phthaloyl acylated chitosan (Kurita et al., 2002b). As the DS value of *N*-phthaloyl acylated chitosan increased, the percentage of decomposition increased and the temperature range over which the decomposition occurred widened. These results indicated that the observed reduction in the thermal stability of *N*-phthaloyl acylated chitosan may result from a weakening of the intra- and inter-molecular hydrogen bonding interactions.

**Table 2**
Yong's modulus and tensile strength of chitosan and *N*-phthaloyl acylated chitosan membranes with different DS values.

| DS | 0 | 2.8 | 3.3 | 3.6 |
|---|---|---|---|---|
| Young's modulus (GPa) | 1.980 | 0.157 | 0.333 | 0.460 |
| Tensile strength (MPa) | 24.600 | 3.750 | 8.880 | 9.060 |

### 3.7. Determination of permeability of urea

Permeability is one of the most important parameters to characterize the controlled-release properties of a membrane. In the current study, urea was selected as a model fertilizer. The accumulated urea penetration across *N*-phthaloyl acylated chitosan membranes with different DS values is shown in Fig. 5. A comparison of the moderately functionalized *N*-phthaloyl acylated chitosan membrane (DS = 2.8) with the chitosan membrane revealed a dramatic decrease of in the total amount of urea released in 6 h from 56,401 to 328 mg. Moreover, the urea permeability of the *N*-phthaloyl acylated chitosan membranes was reduced with the increasing DS value. These results indicated that the introduction of long hydrocarbon chains increased the hydrophobicity of the membrane, which was consistent with the results of the water absorption and contact angle measurements. Furthermore, it is clear from Fig. 5 that all of the curves are linear ($R^2 > 0.99$), suggesting that the permeation rates of the films essentially remain unchanged.

## 4. Conclusions

Novel *N*-phthaloyl acylated chitosan materials have been synthesized using *N*-phthaloyl chitosan as an intermediate, which was subsequently reacted with a long-chain dodecanoyl chloride. The reaction conditions were mild, simple, and more efficient than

those used in other conventional approaches. Furthermore, the DS values were higher and could be adjusted by regulating the dosage of dodecanoyl chloride. The flexibility, film formability, solubility and hydrophobicity of the film had also been significantly improved as a result of the *N*-phthaloyl acylated modifications. Most importantly, the controlled permeability of the membrane could be optimized by adjusting the DS value of the chitosan, representing a significant potential application for the materials in agrochemicals.

## Acknowledgements

This work was supported by the Chinese National Scientific Foundation (21175150), and the National Key Technology R&D Program (2011BAD11B02), of the Ministry of Science & Technology of China.

## References

Abedi-Koupai, J., Varshosaz, J., Mesforoosh, M., & Khoshgoftarmanesh, A. H. (2012). Controlled release of fertilizer microcapsules using Ethylene vinyl Acetate polymer to enhance micronutrient and water use efficiency. *Journal of Plant Nutrition*, *35*, 1130–1138.

Cardenas, G., & Miranda, S. P. (2004). FTIR and TGA studies of chitosan composite films. *Journal of the Chilean Chemical Society*, *49*, 291–295.

Chen, Y., Ding, J., & Qin, W. (2012). Polycation-sensitive membrane electrode for determination of heparin based on controlled release of protamine. *Analyst*, *137*, 1944–1949.

Cunha, A. G., Fernandes, S. C. M., Freire, C. S. R., Silvestre, A. J. D., Neto, C. P., & Gandini, A. (2008). What is the real value of chitosan's surface energy? *Biomacromolecules*, *9*, 610–614.

Feng, F., Liu, Y., Zhao, B., & Hu, K. (2012). Characterization of half *N*-acetylated chitosan powders and films. *Procedia Engineering*, *27*, 718–732.

Fujii, S., Kumagai, H., & Noda, M. (1980). Preparation of poly(acyl) chitosans. *Carbohydrate Research*, *83*, 389–393.

Han, X., Chen, S., & Hu, X. (2009). Controlled-release fertilizer encapsulated by starch/polyvinyl alcohol coating. *Desalination*, *240*, 21–26.

Hiral, A., Odani, H., & Nakajima, A. (1991). Determination of degree of deacetylation of chitosan by $^{1}$H NMR spectroscopy. *Polymer Bulletin*, *26*, 87–94.

Hirano, S., Zhang, M., Chung, B. G., & Kim, S. K. (1999). The *N*-acylation of chitosan fiber and the *N*-deacetylation of chitin fiber and chitin–cellulose blended fiber at a solid state. *Carbohydrate Polymers*, *41*, 175–179.

Huang, R. Y. M., Pal, R., & Moon, G. Y. (1999). Characteristics of sodium alginate membranes for the pervaporation dehydration of ethanol–water and isopropanol–water mixtures. *Journal of Membrane Science*, *160*, 101–113.

Remant Bahadur, K. C., Aryal, S., Bhattarai, S. R., Bhattarai, N., Kim, C. H., & Kim, H. Y. (2006). Stabilization of gold nanoparticles by hydrophobically-modified polycations. *Journal of Biomaterials Science, Polymer Edition*, *17*, 579–589.

Kawashima, T., Nagai, N., Kaji, H., Kumasaka, N., Onami, H., Ishikawa, Y., et al. (2011). A scalable controlled-release device for transscleral drug delivery to the retina. *Biomaterials*, *32*, 1950–1956.

Kurita, K. (1998). Chemistry and application of chitin and chitosan. *Polymer Degradation and Stability*, *59*, 117–120.

Kurita, K., Akao, H., Kobayashi, M., Mori, T., & Nishiyama, Y. (1997). Regioselective introduction of β-galactoside branches into chitosan and chitin. *Polymer Bulletin*, *39*, 543–549.

Kurita, K., Ikeda, H., Yoshida, Y., Shimojoh, M., & Harata, M. (2002). Chemoselective protection of the amino groups of chitosan by controlled phthaloylation: facile preparation of a precursor useful for chemical modifications. *Biomacromolecules*, *3*, 1–4.

Kurita, K., Mori, S., Nishiyama, Y., & Harata, M. (2002). *N*-alkylation of chitin and some characteristics of the novel derivatives. *Polymer Bulletin*, *48*, 159–166.

Li, J., Li, Y., & Dong, H. (2008). Controlled release of herbicide acetochlor from clay/carboxylmethylcellulose gel formulations. *Journal of Agricultural Food Chemistry*, *56*, 1336–1342.

Liu, L., Li, Y., Liu, H., & Fang, Y. (2004). Synthesis and characterization of chitosan-graft-polycaprolactone copolymers. *European Polymer Journal*, *40*, 2739–2744.

Loh, X. J., Peh, P., Liao, S., Sng, C., & Li, J. (2010). Controlled drug release from biodegradable thermo-responsive physical hydrogel nanofibers. *Journal of Controlled Release*, *143*, 175–182.

Lonescu, L. C., Lee, G. C., Sennett, B. J., Burdick, J. A., & Mauck, R. L. (2010). An anisotropic nanofiber/microsphere composite with controlled release of biomolecules for fibrous tissue engineering. *Biomaterials*, *31*, 4113–4120.

Ma, G., Liu, Y., Kennedy, J. F., & Nie, J. (2011). Synthesize and properties of photosensitive organic solvent soluble acylated chitosan derivatives (2). *Carbohydrate Polymers*, *84*, 681–685.

Ma, G., Yang, D., Kennedy, J. F., & Nie, J. (2009). Synthesize and characterization of organic-soluble acylated chitosan. *Carbohydrate Polymers*, *75*, 390–394.

Morimoto, M., Nakao, M., Ishibashi, N., Shigemasa, Y., Ifuku, S., & Saimoto, H. (2011). Synthesis of novel chitosan with chitosan side chains. *Carbohydrate Polymers*, *84*, 727–731.

Muzzarelli, R. A. A. (1996). Chitosan-based dietary foods. *Carbohydrate Polymers*, *29*, 309–316.

Muzzarelli, R. A. A. (2009). Chitins and chitosans for the repair of wounded skin, nerve, cartilage and bone. *Carbohydrate Polymers*, *76*, 167–182.

Osifo, P. O., & Masala, A. (2010). Characterization of direct methanol fuel cell (DMFC) applications with $H_2SO_4$ modified chitosan membrane. *Journal of Power Sources*, *195*, 4915–4922.

Qiu, X., Tao, S., Ren, X., & Hu, S. (2012). Modified cellulose films with controlled permeability and biodegradability by crosslinking with toluene diisocyanate under homogeneous conditions. *Carbohydrate Polymers*, *88*, 1272–1280.

Sreedhar, B., Aparna, Y., Sairam, & Hebalkar, M. N. (2007). Preparation and characterization of HAP/carboxymethyl chitosan nanocomposites. *Journal of Applied Polymer Science*, *105*, 928–934.

Sutton, S., Campbell, N. L., Cooper, A. I., Kirkland, M., Frith, W. J., & Adams, D. J. (2009). Controlled release from modified amino acid hydrogels governed by molecular size or network dynamics. *Langmuir*, *25*, 10285–10291.

Tao, S., Pang, R., Chen, C., Ren, X., & Hu, S. (2012). Synthesis, characterization and slow release properties of O-naphthylacetyl chitosan. *Carbohydrate Polymers*, *88*, 1189–1194.

Thornton, P. D., Mart, R. J., Webb, S. J., & Ulijn, R. V. (2008). Enzyme-responsive hydrogel particles for the controlled release of proteins: designing peptide actuators to match payload. *Soft Matter*, *4*, 821–827.

Tien, C. L., Lacroix, M., Ispas-Szabo, P., & Mateescu, M. A. (2003). *N*-acylated chitosan: hydrophobic matrices for controlled drug release. *Journal of Controlled Release*, *93*, 1–13.

Topacli, C., Topacli, A., Civan, M., Ercan, F., Durmus, M., & Ahsen, V. (2008). Structural characterization of Langmuir–Blodgett films of 4,5-bis (dodecyloxy) phthalic acid. *Thin Solid Films*, *516*, 8299–8306.

Van de Velde, K., & Kiekens, P. (2004). Structure analysis and degree of substitution of chitin, chitosan and dibutyrylchitin by FT-IR spectroscopy and solid state $^{13}$C NMR. *Carbohydrate Polymers*, *58*, 409–416.

Wang, F. L., & Alva, A. K. (1994). Leaching of nitrogen from slow-release urea sources in sandy soils. *Soil Science Society of America Journal*, *60*, 1454–1458.

Wang, J., Lian, Z., Wang, H., Jin, X., & Liu, Y. (2012). Synthesis and antimicrobial activity of Schiff base of chitosan and acylated chitosan. *Journal of Applied Polymer Science*, *123*, 3242–3247.

Wu, L., & Liu, M. (2008). Preparation and properties of chitosan-coated NPK compound fertilizer with controlled-release and water-retention. *Carbohydrate Polymers*, *72*, 240–247.

Xiao, S., Feng, X., & Huang, R. Y. M. (2007). Trimesoyl chloride crosslinked chitosan membranes for $CO_2/N_2$ separation and pervaporation dehydration of isopropanol. *Journal of Membrane Science*, *306*, 36–46.

Zhao, Z., Zheng, J., Wang, M., Zhang, H., & Han, C. (2012). High performance ultrafiltration membrane based on modified chitosan coating and electrospun nanofibrous PVDF scaffolds. *Journal of Membrane Science*, *394–395*, 209–217.

Zong, Z., Kimura, Y., Takahashi, M., & Yamane, H. (2000). Characterization of chemical and solid state structures of acylated chitosans. *Polymer*, *41*, 899–906.

Zou, X. J., Wang, Z. X., Dai, X. M., Zhou, Y., & Ma, X. J. (2006). Rate of controlled release urea pervasion through membrane determined by ultraviolet spectrophotometry. *Spectroscopy and Spectral Analysis*, *26*, 1151–1154 (in Chinese).